



# Dispersal of the radionuclide caesium-137 ( $^{137}\text{Cs}$ ) from point sources in the Barents and Norwegian Seas and its potential contamination of the Arctic marine food chain: Coupling numerical ocean models with geographical fish distribution data



Hilde Elise Heldal\*, Frode Vikebø, Geir Odd Johansen

Institute of Marine Research, PO Box 1870 Nordnes, 5817 Bergen, Norway

## ARTICLE INFO

### Article history:

Received 13 December 2012

Received in revised form

2 April 2013

Accepted 30 April 2013

### Keywords:

Nuclear submarine wrecks

Radioactive contamination

Northeast Arctic cod

Capelin

Ocean model

## ABSTRACT

Dispersal of  $^{137}\text{Cs}$  from the nuclear submarine wrecks *Komsomolets* and *K-159*, which are resting on the seabed in the Norwegian and Barents Seas, respectively, is simulated using realistic rates and hypothetical scenarios. Furthermore, spatiotemporal  $^{137}\text{Cs}$  concentrations in Northeast Arctic cod and capelin are estimated based on survey data. The results indicate that neither continuous leakages nor pulse discharges will cause concentrations of  $^{137}\text{Cs}$  in cod muscle or whole body capelin exceeding the intervention level of 600 Bq/kg fw. Continuous leakages from *Komsomolets* and *K-159* and pulse discharges from *Komsomolets* induced negligible activity concentrations in cod and capelin. A pulse discharge of 100% of the  $^{137}\text{Cs}$ -inventory of *K-159* will, however, result in concentrations in muscle of cod of above 100 times the present levels in the eastern Barents Sea. Within three years after the release,  $^{137}\text{Cs}$  levels above 20 Bq/kg fw in cod are no longer occurring in the Barents Sea.

© 2013 Elsevier Ltd. All rights reserved.

## 1. Introduction

Radioactive contaminants have been present in the Arctic marine environment for more than 50 years. An updated overview of the most important sources is available in AMAP (2009). The present levels in biota, seawater and sediments in the Barents Sea and adjacent areas are low (e.g., NRPA, 2011; Gwynn et al., 2012). For example, the levels of caesium-137 ( $^{137}\text{Cs}$ ) in muscle of cod (*Gadus morhua* L.) in the Barents Sea have decreased from 0.5 to 1 Bq/kg fresh weight (fw) in the early 1990s to the current level of 0.1–0.2 Bq/kg fw. In comparison, an intervention level for the activity concentration of  $^{137}\text{Cs}$  in food, such as muscle of cod, was set to 600 Bq/kg fw by the Norwegian authorities after the Chernobyl accident in 1986.

Around the turn of the millennium, many researchers predicted the environmental impact of potential radioactive leakages from specific point sources, e.g., Baxter et al. (1998); dump sites in the Kara Sea, Blindheim et al. (1994) and Høibråten et al. (2003) (submarine *Komsomolets*) and Amundsen et al. (2002); submarine

*Kursk*, which was raised in October 2001). The outcome of the predictions differs for each source. Blindheim et al. (1994) and Høibråten et al. (2003) concluded that *Komsomolets* represents a minor radioactive pollution problem, partly because of the great depth at which the wreck is located (1655 m). Baxter et al. (1998) concluded that the resultant doses from radioactive leakages from dump sites in the Kara Sea are negligible on regional and global scales. However, maximum individual doses could reach higher levels than the limit recommended for the public (1 mSv year<sup>-1</sup>) on a local scale (e.g., in Abrosimov Bay), but this scenario is regarded as less serious because the bay areas are uninhabited. A source that has obtained less attention than the above-mentioned is the Russian nuclear submarine *K-159*, which rests at a depth of 238 m outside of the Murmansk Fjord. This area represents important habitats for commercial fish stocks, e.g., as a spawning and nursery area for capelin (*Mallotus villosus* Müller, 1776) (Hamre, 1994; Sakshaug et al., 1994; Olsen et al., 2010).

The present study assesses the effect of potential long-term leakages and pulse releases of  $^{137}\text{Cs}$  from *Komsomolets* and *K-159*, on fisheries resources in the Barents Sea and adjacent areas. The fisheries resources studied here are limited to Northeast Arctic cod and capelin during the autumn and winter, both in the pelagic and benthic parts of the water masses. The approach is generic and

\* Corresponding author.

E-mail address: [hilde.elise.heldal@imr.no](mailto:hilde.elise.heldal@imr.no) (H.E. Heldal).

involves an estimate of the 3-dimensional (3D) dispersal of particles; it represents potential discharges of  $^{137}\text{Cs}$  by utilising a numerical ocean model and quantifies the overlap with the observed geographical fish distribution data. Specifically, we would like to answer the following questions: 1) What are the expected activity concentrations of  $^{137}\text{Cs}$  in muscle of cod and whole-body capelin given the specific levels of long-term or pulse leakages? 2) How does the concentration of  $^{137}\text{Cs}$  in seawater vary spatially and temporally in relation to the timing and location of the discharges? 3) Will the levels of  $^{137}\text{Cs}$  in cod and capelin exceed the intervention level of 600 Bq/kg fw?

## 2. Methods

### 2.1. The choice of $^{137}\text{Cs}$ as the studied radionuclide

We chose to focus on  $^{137}\text{Cs}$  because it is one of the two predominant radionuclides in terms of total activity in the *Komsomolets* and *K-159* reactors (the other radionuclide is  $^{90}\text{Sr}$ ; Høibråten et al., 1997, 2003; Hermansen et al., 2006) and because  $^{137}\text{Cs}$  is the radionuclide expected to have the largest impact on the marine ecosystem. The potential magnitude of this impact is due to the relatively long half-life ( $t_{1/2} = 30$  years) of  $^{137}\text{Cs}$ , its potential to be transported with ocean currents over large distances, and its transferability through the marine food chain (Avery, 1996; Heldal et al., 2003).

### 2.2. The point sources and the dominant circulation patterns near the sources

*Komsomolets* and *K-159* are comparable with respect to radionuclide inventory, but located in different marine environments, which may greatly affect a potential discharge. *Komsomolets* sank on April 7th, 1989, and it is now lying at a depth of 1655 m at 73°43'16"N and 13°16'52"E in the Norwegian Sea (Høibråten et al., 1997, 2003, Fig. 1). Gladkov and Sivintsev (1994) and Høibråten et al. (1997, 2003) estimated the 1989 content of  $^{137}\text{Cs}$  as  $3.1 \cdot 10^{15}$  Bq, which is used in the scenarios for the present study. *K-159* sank on August 31st, 2003, three nautical miles northwest of the island of Kildin outside of the Murmansk Fjord at a depth of 238 m (Hermansen et al., 2006, Fig. 1). Compared to *Komsomolets*, much less information concerning *K-159* is publicly available. The Norwegian Radiation Protection Authority (NRPA) has estimated that the total radionuclide inventory of *K-159* in 2003 was between  $3 \cdot 10^{15}$

and  $13 \cdot 10^{15}$  Bq (Hermansen et al., 2006) and that the  $^{137}\text{Cs}$  and  $^{90}\text{Sr}$  content each accounted for more than 40% of the total inventory. 40% of the total inventory equals to  $1.2 \cdot 10^{15}$ – $5.2 \cdot 10^{15}$  Bq for  $^{137}\text{Cs}$ . We use the latter concentration in the scenarios in the present study.

*Komsomolets* is located in the continental slope between the shallow Barents Sea (average depth of approximately 230 m) and the deep Norwegian Sea (depth of more than 2000 m). The bottom topography and main currents in the area lead toward the Fram Strait, which connects the Nordic Seas and the Arctic Oceans. The dominating flow direction at greater depths of the slope is expected to be north, but little is known concerning its variability in direction and strength. To the southeast of the site, the Bear Island Trough penetrates the shelf of the Barents Sea. Importantly, this opening is shallower than 500 m and is mainly downstream of this point source. The northward flowing Norwegian Atlantic Slope Current (NASC, temperature  $> 0^\circ\text{C}$  and salinity  $> 35$ ) trapped along the Norwegian continental slope bifurcates at the southern slope of the Bear Island Trough. One branch enters the Barents Sea, and the other branch flows west of Spitsbergen toward the Fram Strait. The eastward flowing branch of the NASC enters the southwestern Barents Sea, with the fresh wedge-shaped Norwegian Coastal Current (NCC) trapped between the NASC and the Norwegian Coast. The circulation pattern near *K-159* is governed by the topography, although the degree depends on the vertical density profile. A strong density gradient may decouple the upper mixed layer and the water below. The currents are rich in mesoscale features at different spatial scales due to the numerous banks and troughs.

### 2.3. The ocean model ROMS and the transport of particles

The spatiotemporal distribution of  $^{137}\text{Cs}$  was simulated with daily mean output of the 3D numerical ocean model ROMS (Regional Ocean Modeling System) ([www.myroms.org](http://www.myroms.org); Haidvogel et al., 2008) covering the period 1989 until 2008. The model domain is shown in Fig. 1 and is covered by a 4 by 4 km horizontal grid, with 30 sigma-coordinate levels in the vertical. Monthly mean lateral boundary conditions are taken from a global ROMS simulation of 20 by 20 km horizontal resolution, and atmospheric momentum and heat fluxes from ERA40 interim ([www.ecmwf.int](http://www.ecmwf.int)). Further details of the model setup and comparison with hydrographic and current meter measurements along the Norwegian Coast can be found in Vikebø et al. (2010).

Under the assumption that all  $^{137}\text{Cs}$  discharged from *Komsomolets* and *K-159* is dissolved in seawater, the dispersal was modelled by a Lagrangian particle-tracking model (Ramsden and Holloway, 1991) allowing us to follow individual pollution plume parcels. We released a large number of particles (pollution plume parcels),

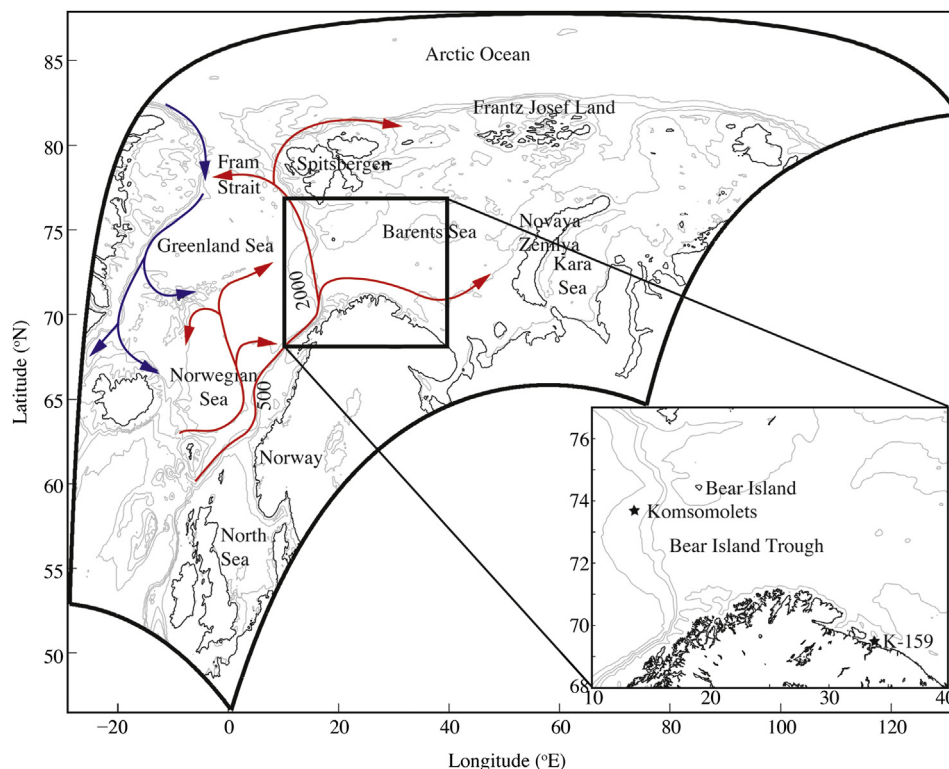


**Fig. 1.** Model domain covering the Nordic, North, Barents and Kara Seas and parts of the Arctic Ocean. Contours indicate depths of 30, 200, 500, 1000 and 2000 m. The inset shows the positions of the two sunken submarines.

either as a continuous leakage or as a pulse discharge at the point sources, to model the dispersal of  $^{137}\text{Cs}$ . The particles were advected with the daily mean depth-dependent horizontal velocities of the ocean model. The displacement of particles is accomplished with a 4<sup>th</sup>-order Runge-Kutta advection scheme (Ramsden and Holloway, 1991) and bilinear 3D interpolation of the daily mean velocities. Vertical movement of  $^{137}\text{Cs}$  is simulated by utilizing the binned random walk scheme as presented in Thygesen and Adlandsvik (2007) together with turbulence calculated in ROMS in every grid cell at every vertical layer. The water column is divided into 5-m bins and the scheme allows particles to jump between adjacent bins in accordance with the level of turbulence within their present bins. Even if the vertical eddy diffusivity coefficient varies with depth, this ensures a convergence toward homogeneous vertical distribution of a neutral tracer with time, as is the case with  $^{137}\text{Cs}$ . The only effect of varying vertical eddy diffusivity is that diffusion through layers of low-level turbulence is slower than that through the layers of high-level turbulence.

### 2.3.1. Experiments A and B

The numerical simulations are continuous leakages (Experiment A) and pulse discharges (Experiment B) from the two point sources.

In Experiment A, we released 100 particles every day for 5 years at the locations of *Komsomolets* and *K-159* from April 7th, 1989 and August 31st, 2003, respectively. In total, this process yields 36,500 particles per year.

Russian investigations of the wreck of *Komsomolets* in the early 1990s revealed a leakage of radionuclides through a ventilation pipe (Gladkov and Sivintsev, 1994; Høibråten et al., 1997, 2003). The  $^{137}\text{Cs}$  activity concentration inside the ventilation pipe was measured *in situ* and found to be on the order of 1 MBq/m<sup>3</sup>. Water-flow measurements inside the ventilation pipe indicated maximum yearly releases of  $^{137}\text{Cs}$  from *Komsomolets* to be between 370 and 500 GBq/year. We have used 500 GBq/year in the present study, thought to represent a worst case scenario. Because no such information is available for *K-159*, we used the same value for this submarine; therefore, each particle represents approximately  $1.37 \cdot 10^7$  Bq.

In Experiment B, we released 50,000 particles instantaneously on April 7th, 1989 for *Komsomolets* and on August 31st, 2003 for *K-159*. We only considered a single-pulse discharge of 100% of the total inventory of  $^{137}\text{Cs}$  from both submarines. Assuming  $3.1 \cdot 10^{15}$  Bq  $^{137}\text{Cs}$  in *Komsomolets*, each particle represents  $6.2 \cdot 10^{10}$  Bq. Likewise, assuming  $5.2 \cdot 10^{15}$  Bq in *K-159*, each particle represents  $10.4 \cdot 10^{10}$  Bq (the inventories are in accordance with Section 2.2).

The dates in Experiment A and B are arbitrarily chosen as the dates at which the submarines sank, although there is no evidence that substantial leakages occurred at that time.

We quantify the level of Bq/m<sup>2</sup> of surface (integrated over the entire water column) to visualise transport patterns. Additionally, we quantify the level of Bq/m<sup>3</sup> for the upper and lower 50 m of water column on February 15th and September 1st (the time of the fish sampling, see Section 2.5) for 5 years following the discharges to calculate  $^{137}\text{Cs}$  concentrations in fish. The calculation is performed following the  $^{137}\text{Cs}$  release every year by summarising the number of particles in each 4 by 4 km grid. Because this task is performed for the purpose of overlap estimates with cod and capelin, we did not consider depths below 500 m, i.e., if the water depths were below 500 m, we considered that the bottom part of the water column occurred from 450 to 500 m.

### 2.4. Concentrations of $^{137}\text{Cs}$ in fish

To calculate the  $^{137}\text{Cs}$  concentrations in cod and capelin, we used concentration factors (CFs). The CF for a given species equals the concentration per unit mass of organism (Bq/kg fw) divided by the concentration per unit volume of seawater (Bq/L) under equilibrium conditions (IAEA, 2004). This equilibrium based approach may, however, introduce a significant uncertainty. This is discussed in Section 4.2.

The CFs used in the present study, 73 for cod and 17 for whole-body capelin, are average values based on a dataset specific for the Norwegian and Barents Seas (Heldal et al., 2003). Thus, regardless of the estimated ambient seawater  $^{137}\text{Cs}$  concentration, the concentration of  $^{137}\text{Cs}$  in muscle of cod is 73 times greater.

### 2.5. Fish survey data

Cod and capelin were chosen as representatives of the biota exposed to radioactive contamination. These two species are important ecologically as well as commercially and have a wide geographic distribution and migration pattern in the Barents Sea (Bergstad et al., 1987; Hamre, 1994). These species are also well described by survey data at different times of the year and at different life history stages. Geographic distribution data for cod and capelin were obtained from yearly routine scientific surveys conducted as a cooperative effort through a partnership between the Institute of Marine Research (IMR, Norway) and the Polar Research Institute of Marine Fisheries and Oceanography (PINRO, Russia) in winter and autumn, which corresponds to the model fields from February 15th and September 1st. We used data from two periods, 1990–1998 and 2004–2008, which correspond to the timing of the two submarine accidents and the subsequent transport of radionuclides in the particle-tracking model.

Geographic distribution data for the first year of life for cod and capelin were taken from the 0-group surveys (international pelagic juvenile fish surveys in the Barents Sea where the fish species are sampled at the end of the period of pelagic free drift about 5 months after spawning) in late August/early September. These surveys are based on catches from pelagic trawl, and the distributions are representative from approximately 0–50 m depth. The abundance per trawl station is calculated as swept area estimates. Detailed descriptions of survey methodology and data analyses can be found in Dingsør (2005) and Eriksen et al. (2009).

Geographic distribution data for adolescent and adult cod were taken from annual demersal fish surveys in January/March and August/October. These surveys are based on catches from bottom trawl, and the distributions are representative for the bottom layer to approximately 50 m above. The winter survey is a combined acoustic and bottom trawl synoptic survey that has been performed in January/March since 1981.

The fish data were split into two size groups: the <45 cm size group, which represents the fish that are not targeted by commercial fisheries and the ≥45 cm size group, which represents the targeted portion of the stock. All of the bottom trawl data for cod were calculated as swept area estimates per trawl haul, and the unit was the number of fish per square nautical mile. The survey methodologies are detailed by Jakobsen et al. (1997).

Geographic distribution data for adolescent and adult capelin were obtained from regular acoustic fish surveys in August and October. These surveys are based on recordings from scientific echosounders, recalculated to fish densities and distributed over age groups based on biological samples. The distributions were aggregated for all of the age groups and assumed to be representative from a depth of approximately 0 m–50 m. The Norwegian-USSR acoustic survey of the Barents Sea has been conducted annually between August and October since 1972. The computation of fish abundance is standard for acoustic surveys, and the unit of measure is the number of fish (N) per square nautical mile. It is given as N°10 Exp-7. The survey methodologies are detailed by Gjosæter et al. (1998).

Due to variation in design, varying coverage in time and space, differences in equipment and methodology, weather conditions, political constraints and technical problems and development, the fish distribution data must be viewed as indicative rather than absolute measures of abundance.

### 2.6. Coupling of the simulated spatiotemporal $^{137}\text{Cs}$ distribution with fish survey data

To quantify the overlap between the simulated concentrations of  $^{137}\text{Cs}$  in seawater and fish, we compiled both the particle model output and the fish survey data in a common  $25 \times 25$  km regular grid covering the Barents Sea (Westgård et al., 2010). The projection is the Lambert Azimuthal Equal Area. The grid is 2100 km in the x-direction (west–east), corresponding to 84 squares, and 2000 km in the y-direction (south–north), corresponding to 80 squares, with the centre position at 75°N and 35°E. Observations of fish abundance were reported as the density of fish within each grid cell. This measure enabled us to also consider the abundance of fish in addition to the area overlap. For the purpose of the following discussion, overlap is reported as the fraction of the fish distribution containing levels of  $^{137}\text{Cs}$  exceeding 0.2 Bq/kg fw. This equals the current contamination level in cod in the Norwegian and Barents Seas, which has been stable or slightly decreasing for the last decade (Gwynn et al., 2012; NRPA, 2011).

## 3. Results

The results are divided into three main sections. First, we present the main features of the dispersion of  $^{137}\text{Cs}$  from the two sources, both for continuous leakages and for pulse discharges.

Second, we present isolines for  $^{137}\text{Cs}$  concentrations in cod following a pulse discharge of the total inventory from *K-159*, assuming that cod is present everywhere. Continuous leakages from *Komsomolets* and *K-159* and pulse discharges from *Komsomolets* induced negligible activity concentrations of  $^{137}\text{Cs}$  in cod and capelin. We therefore only present maps showing the main features of dispersion for these cases.

Finally, we present the per cent overlap between different life stages of observed cod and capelin with three different  $^{137}\text{Cs}$  levels, after the pulse discharge of the total  $^{137}\text{Cs}$  inventory of *K-159*. Only the pulse discharge from the *K-159* resulted in significantly increased  $^{137}\text{Cs}$  levels in fish. Consequently, the overlap analyses are only presented for this particular experiment.

Neither continuous leakages nor pulse discharges of  $^{137}\text{Cs}$  from *Komsomolets* and *K-159* yield activity concentrations above the intervention level of 600 Bq/kg fw in cod and capelin.

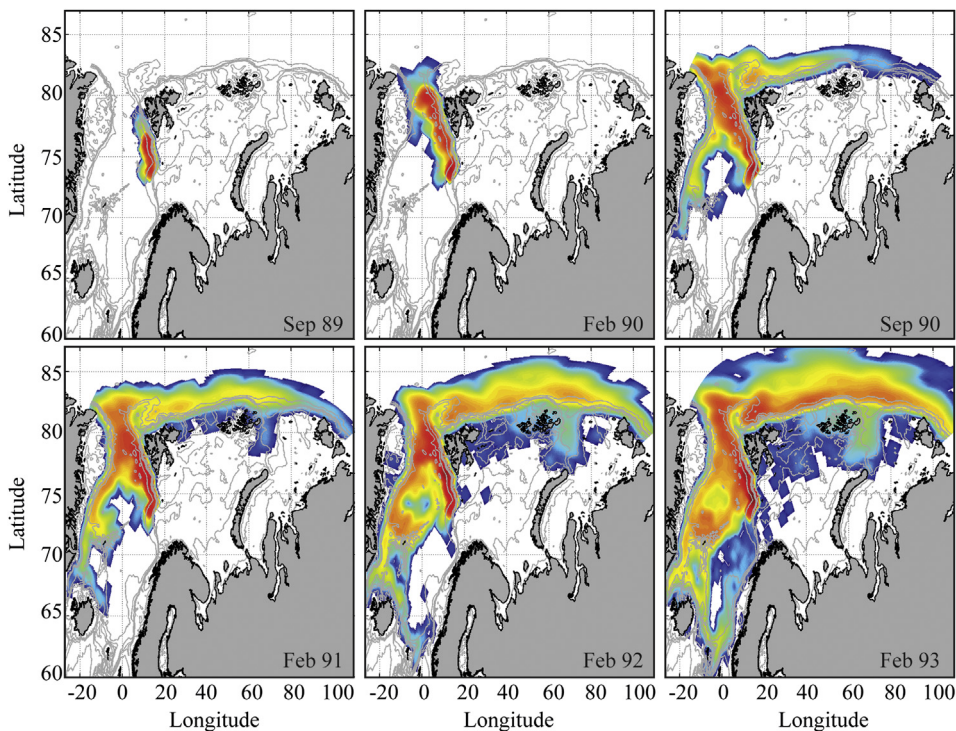


**Fig. 2.** Bq/m<sup>2</sup> surface at different times after a continuous leakage of <sup>137</sup>Cs from *Komsomolets* on April 26th, 1989. The colour scale is logarithmic and indicates levels from –3.5 (blue) to 1.5 (red). (For interpretation of the references to colour in this figure legend, the reader is referred to the web version of this article.)

3.1. Experiment A

Figs. 2 and 3 show Bq/m<sup>2</sup> surface water following a continuous release of 500 GBq/year for *Komsomolets* and *K-159*, respectively.

The discharge from *Komsomolets* is either re-circulated in the Fram Strait and transported southward in the East Greenland Current or transported into the Arctic Ocean and eastward along the shelf edge. The part flowing south along East Greenland is re-circulated

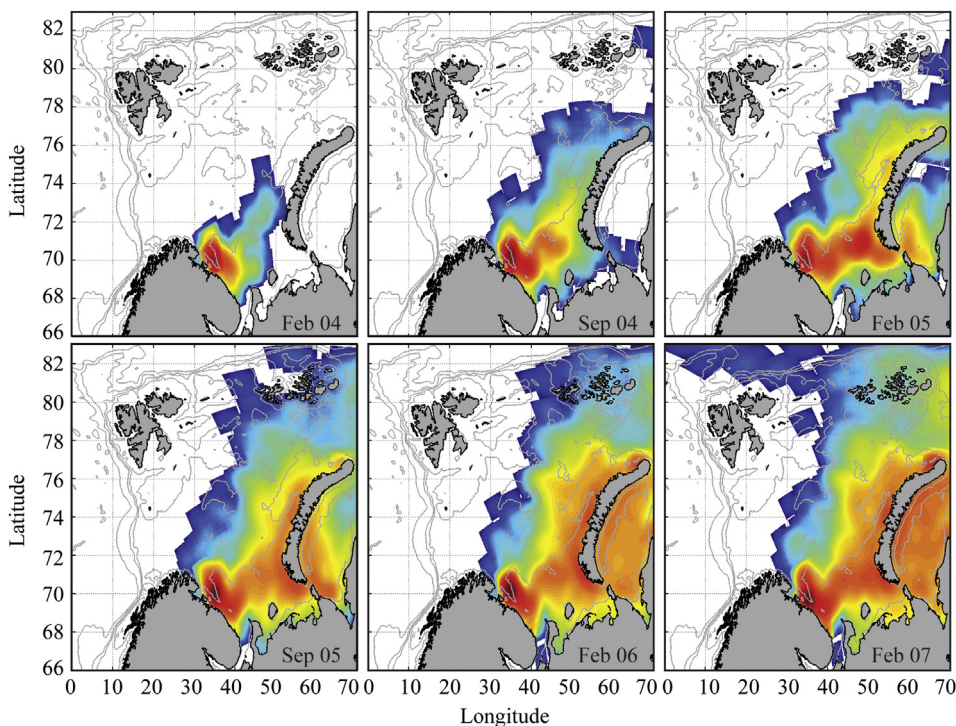


**Fig. 3.** Bq/m<sup>2</sup> surface at different times after a continuous leakage of <sup>137</sup>Cs from *K-159* on August 31st, 2003. The colour scale is logarithmic and indicates levels from –3.5 (blue) to 1.5 (red). (For interpretation of the references to colour in this figure legend, the reader is referred to the web version of this article.)

in the Greenland Sea, re-circulated in the Norwegian Sea, or advected out of the Norwegian Sea through the Denmark Strait. Only a minor part of the discharge flows into the Barents Sea, and it only flows southward on the eastern side of Spitsbergen. The maximum concentrations are reached soon after the discharge and kept at a level of some tens of Bq/m<sup>2</sup> of surface. The discharge from *K-159* spreads northeast toward Novaya Zemlya and farther into the Kara Sea either on the southern or northern passage of Novaya Zemlya. Dispersion to the northern and western parts of the Barents Sea is limited.

### 3.2. Experiment B

Pulse discharges of 100% of the total inventory of <sup>137</sup>Cs from *Komsomolets* and *K-159* are shown in Figs. 4 and 5, respectively. A pulse discharge from *Komsomolets* spreads in the same way as the continuous leakages, but the maximum values of Bq/m<sup>2</sup> of surface occur shortly after the release in a narrow band stretching downstream of the source. After several years, the highest values are found in the Greenland Sea and along the shelf edge of the Arctic Ocean north of the Barents Sea. A pulse discharge from *K-159* also spreads in the same way as the continuous leakages but with much greater amounts of <sup>137</sup>Cs. Maximum values are on the order of 100,000 Bq/m<sup>2</sup> of surface in a water column of approximately 200 m, which corresponds to a concentration of about 500 Bq/m<sup>3</sup> if <sup>137</sup>Cs is evenly distributed in the water column. Values on the order of 100,000 Bq/m<sup>2</sup> of surface still occur in the Kara Sea at 5 years after the release. Only low values occur in the northwestern Barents Sea, and negligible values occur in the southwestern Barents Sea.

### 3.3. <sup>137</sup>Cs in cod assuming cod is present everywhere

Isolines for <sup>137</sup>Cs concentrations in cod of 1 (black), 10 (green) and 100 (red) times 0.2 Bq/kg fw near the surface and near the

bottom, assuming that cod is present everywhere, are shown in Fig. 6 and Fig. 7, respectively, for the release of the total inventory of <sup>137</sup>Cs in *K-159*. Note that the <sup>137</sup>Cs already present in the Barents Sea is not included in these results.

Maximum <sup>137</sup>Cs concentrations in cod are 63 and 123 Bq/kg fw in the near-surface and near-bottom layer, respectively. The <sup>137</sup>Cs concentrations in capelin are a factor of 4.3 lower. Within three years after the release, <sup>137</sup>Cs levels above 20 Bq/kg in cod (100 times the general contamination level of 0.2 Bq/kg fw) near the surface are no longer occurring in the Barents Sea. However, near the bottom such levels of <sup>137</sup>Cs disappear within the first year. Notably, <sup>137</sup>Cs is vertically neutral, and in a shallow shelf sea such as the Barents Sea, <sup>137</sup>Cs requires more time to spread into channels and troughs located behind ridges and seamounts than near the surface, where there are fewer obstacles. Consequently, higher levels of Bq/kg cod are found near the surface than near the seabed from February 2005 and later. The corresponding isolines for capelin will cover a much smaller geographic area as the CF for capelin is about 23% of that for cod (figures are not included).

### 3.4. Overlap of different life stages of observed cod and capelin with <sup>137</sup>Cs

The overlap of different life stages of observed cod and capelin with the <sup>137</sup>Cs levels exceeding 0.2 Bq/kg fw by 1, 10 and 100 times for September and February up to 5 years after the discharge of 100% of the total inventory of <sup>137</sup>Cs in *K-159* are presented in Table 1.

Large cod occupying the bottom 50 m in September 2004, one year after the pulse discharge, represent the highest degree of overlap with <sup>137</sup>Cs levels exceeding 0.2 Bq/kg fw (48.6%). The values drop to 39.5 and 6.9% for overlap with <sup>137</sup>Cs levels exceeding 10 and 100 times the present contamination level, respectively. Small cod in February about 1.5 years after the discharge represent the second largest overlap, with maximum values of 42.6%, increasing from the

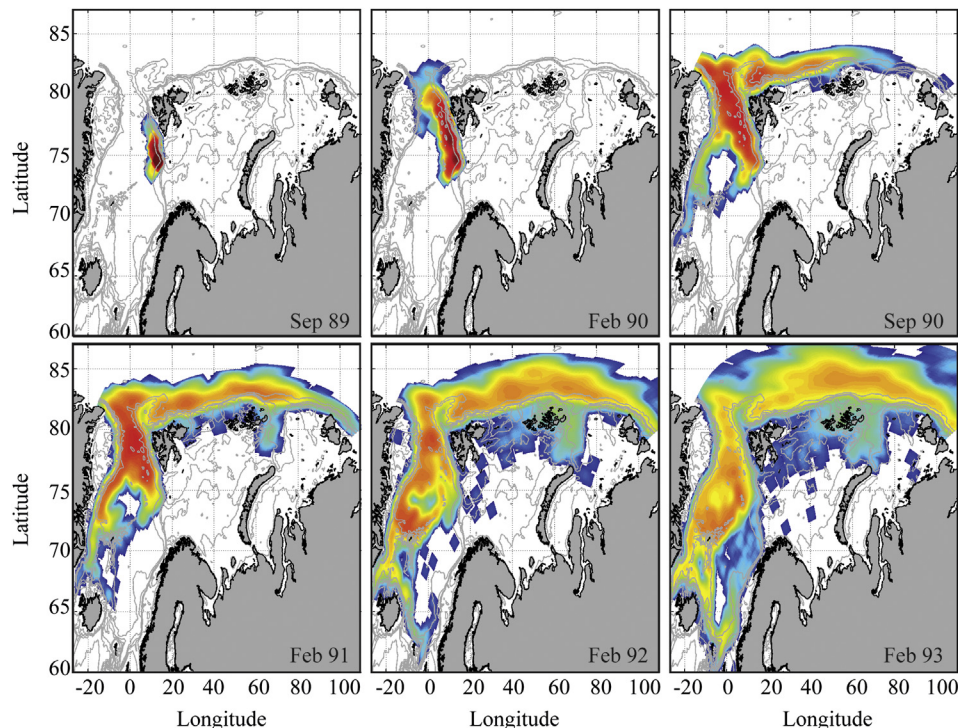
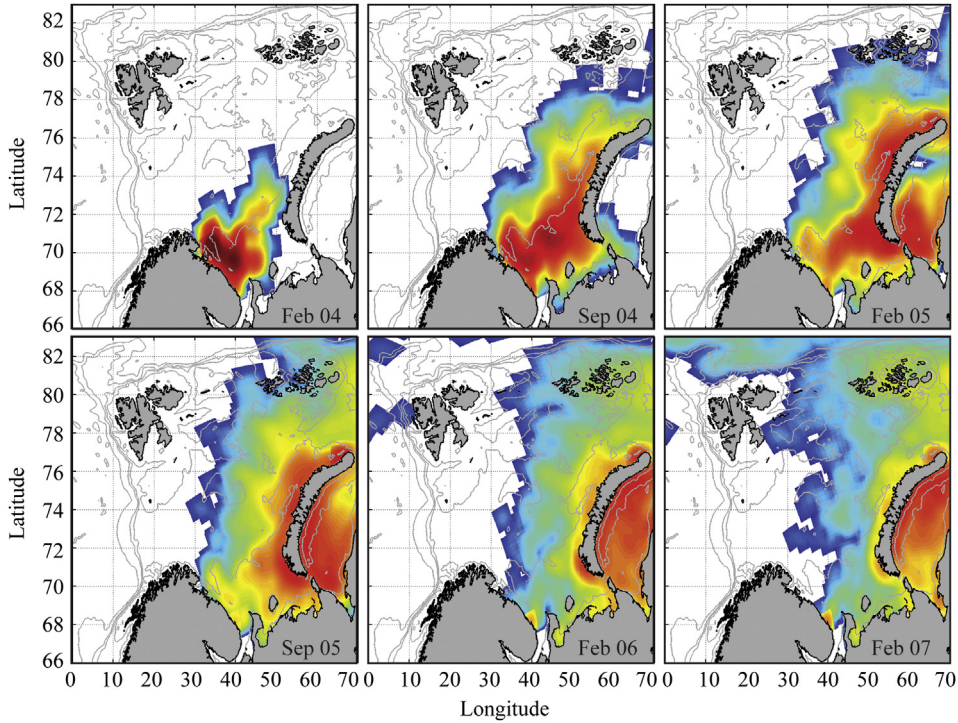


Fig. 4. Bq/m<sup>2</sup> surface at different times after a pulse discharge of 100% of the total inventory of <sup>137</sup>Cs from *Komsomolets* on April 26th, 1989. The colour scale is logarithmic and indicates levels from 0 (blue) to 5 (red). (For interpretation of the references to colour in this figure legend, the reader is referred to the web version of this article.)



**Fig. 5.** Bq/m<sup>2</sup> surface at different times after a pulse discharge of 100% of the total inventory of <sup>137</sup>Cs from K-159 on August 31st, 2003. The colour scale is logarithmic and indicates levels from 0 (blue) to 5 (red). (For interpretation of the references to colour in this figure legend, the reader is referred to the web version of this article.)

year before, half a year after the discharge, with an overlap of 30.1%. 0-gr. capelin occupying the upper 50 m in February represent the third largest overlap, with maximum values of 42.0% after approximately 1 years following the discharge. Further, the 0-group capelin have a higher overlap with levels of <sup>137</sup>Cs exceeding 0.2 Bq/

kg fw after approximately 1 year compared to the older capelin, with maximum values of 6.6%. However, the overlap estimate increases to 19.9% for adult capelin in the following year, which is greater than for the 0-group capelin (17.9%). Three years after the discharge, the capelin and cod of all of the year classes have very

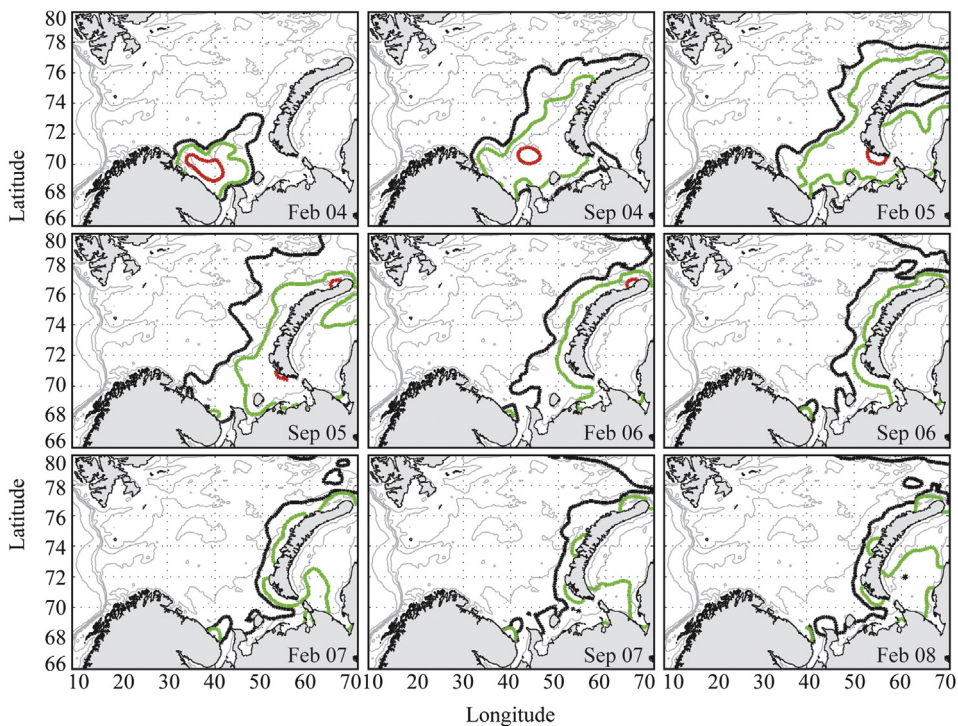


**Fig. 6.** Isolines for levels of <sup>137</sup>Cs in cod near the surface that exceed 1 (black), 10 (green) and 100 (red) times the current observed levels of 0.2 Bq/kg fw at different times after a pulse discharge of <sup>137</sup>Cs from K-159 on August 31st, 2003. (For interpretation of the references to colour in this figure legend, the reader is referred to the web version of this article.)

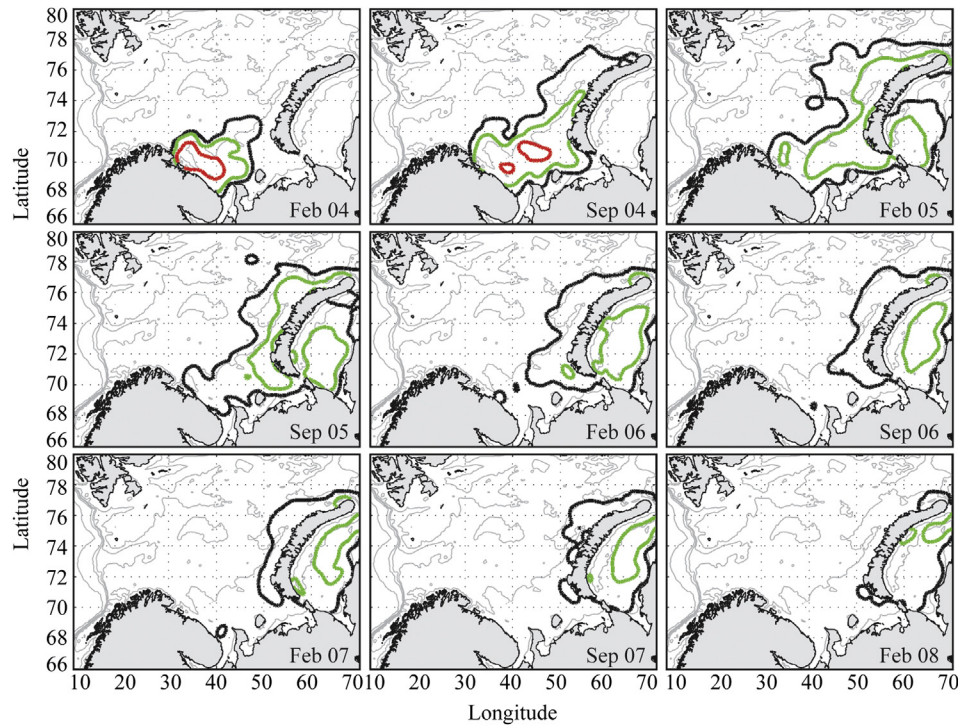


**Fig. 7.** Isoline for levels of  $^{137}\text{Cs}$  in cod near the bottom that exceed 1 (black), 10 (green) and 100 (red) times the current observed levels of 0.2 Bq/kg fw at different times after a pulse discharge of  $^{137}\text{Cs}$  from K-159 on August 31st, 2003. (For interpretation of the references to colour in this figure legend, the reader is referred to the web version of this article.)

little or no overlap with  $^{137}\text{Cs}$  levels exceeding 2 Bq/kg fw (10 times the present contamination level).

#### 4. Discussion

##### 4.1. Modelling the dispersion of conservative radionuclides from point sources

Numerical models have been used to simulate the dispersion of various conservative radionuclides (e.g.,  $^{99}\text{Tc}$ ,  $^{125}\text{Sb}$ ,  $^{129}\text{I}$  and  $^{137}\text{Cs}$ )

**Table 1**

The overlap of different life stages of observed cod and capelin with the  $^{137}\text{Cs}$  levels corresponding to 1, 10 and 100 times the current level of 0.2 Bq/kg fw for September and February up to 5 years after the discharge of the total inventory of  $^{137}\text{Cs}$  in K-159.

|                         |     | 2004 | 2005 | 2006 | 2007 | 2008 |
|-------------------------|-----|------|------|------|------|------|
| Large cod September     | 1   | 48.6 | 0.4  | 9.4  | 7.8  | 3.2  |
|                         | 10  | 39.5 | 0.0  | 0.0  | 0.0  | 0.0  |
|                         | 100 | 6.9  | 0.0  | 0.0  | 0.0  | 0.0  |
| Small cod September     | 1   | 28.1 | 2.4  | 4.5  | 3.5  | 2.5  |
|                         | 10  | 18.8 | 0.0  | 0.0  | 0.0  | 0.0  |
|                         | 100 | 3.5  | 0.0  | 0.0  | 0.0  | 0.0  |
| Large cod February      | 1   | 16.9 | 28.0 | 2.6  | 0.0  | 0.0  |
|                         | 10  | 10.0 | 1.9  | 0.0  | 0.0  | 0.0  |
|                         | 100 | 3.6  | 0.0  | 0.0  | 0.0  | 0.0  |
| Small cod February      | 1   | 30.1 | 42.6 | 11.5 | 0.0  | 0.0  |
|                         | 10  | 14.5 | 16.2 | 0.0  | 0.0  | 0.0  |
|                         | 100 | 4.1  | 0.0  | 0.0  | 0.0  | 0.0  |
| Total capelin September | 1   | 6.6  | 19.9 | 0.3  | 0.3  | 0.1  |
|                         | 10  | 3.7  | 5.4  | 0.0  | 0.0  | 0.0  |
|                         | 100 | 0.0  | 0.0  | 0.0  | 0.0  | 0.0  |
| 0-gr. capelin September | 1   | 42.0 | 17.9 | 3.9  | 1.5  | 1.2  |
|                         | 10  | 11.9 | 1.5  | 0.4  | 0.0  | 0.0  |
|                         | 100 | 0.0  | 0.0  | 0.0  | 0.0  | 0.0  |
| 0-gr. cod September     | 1   | 29.5 | 11.4 | 3.6  | 1.7  | 4.3  |
|                         | 10  | 19.3 | 2.4  | 0.0  | 0.0  | 0.7  |
|                         | 100 | 3.9  | 0.3  | 0.0  | 0.0  | 0.0  |

from point sources in the North and Nordic Seas for several decades. The dispersion of known amounts of radionuclides discharged from Sellafield and La Hague have been the most investigated cases (e.g., Hallstadius et al., 1987; Schönfeld, 1995; Breton and Salomon, 1995; Gao et al., 2004; Karcher et al., 2004; Alfimov et al., 2006; Orre et al., 2007), as the results from these studies may be compared and calibrated with observed data.

The ocean models used in the studies above represent a wide range of approaches, from simple compartment models with fixed tracer fluxes across boundaries to sophisticated state-of-the-art isopycnal models covering the entire North Atlantic and the Arctic. Additionally, the horizontal resolution is highly variable, but the models covering the Nordic Seas and the Barents Sea have a resolution of 20 km or more. Clearly, this resolution is not sufficient to resolve mesoscale features along the Norwegian Coast or in the Barents Sea and will result in an underestimation of the horizontal diffusion. In contrast, the ROMS model used in the present study is a state-of-the-art 3D model with terrain-following vertical coordinates setup with a horizontal resolution of 4 km. However, available computational resources limit the possibilities of including ensemble members enabling uncertainty estimates with high-resolution applications and a high number of particles to represent the spread of radioactivity. The baroclinic Rossby radius of deformation is approximately 5 km along the Norwegian Coast and into the Barents Sea (Hansen and Samuelsen, 2009). Hence, the resolution only partly resolves physical features where rotation effects become as important as buoyancy effects (Gill, 1982). The underestimation of horizontal diffusion, though less severe than for models of coarser grids, may be partly solved by including artificial isotropic diffusion in the form of a random walk to compensate for the lack of sub-grid scale mixing. We have chosen not to do this because we believe that this deficiency does not significantly affect our dispersal estimate, and if we were to try to parameterise the underestimation of horizontal diffusion, a direction-independent

random walk is not a realistic solution for a shelf sea close to the coast (Vikebø et al., 2007).

#### 4.1.1. Dispersion from Komsomolets

The results found in the present study are in accordance with Blindheim et al. (1994). Both studies show that a radioactive leakage from *Komsomolets* will have an insignificant impact on fish and other marine resources in the Barents Sea because a very small portion of the contamination will enter this area, and in doing so, only in the northern parts. The present study shows that this applies both for continuous leakages and pulse discharges. Further, because of the great depth at which the wreck lies, the contamination will be diluted to low levels before reaching the upper mixed layers.

#### 4.1.2. Dispersion from K-159

If the daily rate of a continuous leakage corresponding to a yearly release of 500 GBq were distributed in a cylinder of radius 1000 m and height of 100 m, this would give concentrations in seawater of approximately 4.36 Bq/m<sup>3</sup>. Using the CF for cod of 73 (see Section 2.4), the calculation yields concentrations in cod of 0.32 Bq/kg fw, respectively, which is about 60% above the current observed level of <sup>137</sup>Cs in cod. We have not been able to find results from other dispersion studies of radionuclides from *K-159* in the literature.

In contrast, a pulse discharge of the total inventory of *K-159* would lead to <sup>137</sup>Cs levels exceeding the present contamination level in fish in most of the eastern Barents Sea for several years. A considerable fraction of the fish would even be contaminated at levels above 10–100 times this, though limited to the first three years.

Our results illustrate that potential activity concentrations in cod and capelin is sensitive to the localisation of a discharge. Clearly, *K-159* is situated so that most of a leakage would flow into the Kara Sea either through the Kara Gate Strait in the south or between Novaya Zemlya and Frantz Josef Land to the north (see Fig. 5). Other marine organisms distributed in the eastern part of the Barents Sea and the Kara Sea may also be contaminated by discharges from *K-159*. Consequently, because observational availability restricts the assessment to cod and capelin, one may underestimate the overall impact of discharges of radionuclides on the Barents Sea ecosystem.

#### 4.2. Simplifications and constraints in the study design

Caesium-137 is widely used as an oceanographic tracer (e.g., Kershaw and Baxter, 1995; Smith et al., 1998) and is considered to have a conservative behaviour in seawater. However, it is well known that a minor fraction of <sup>137</sup>Cs binds to sediments. In sediments in the Norwegian and Barents Sea, we typically find <sup>137</sup>Cs-levels up to approximately 5 Bq/kg (e.g., Heldal et al., 2002; NRPA, 2011). In the present study, we assume that all of the <sup>137</sup>Cs discharged from *Komsomolets* and *K-159* is dissolved in seawater as ions and is available for uptake in cod and capelin. This particular simplification will lead to an overestimation of the <sup>137</sup>Cs concentrations in cod and capelin.

Further, we have not accounted for radioactive decay during the time span of the model period. The half-life ( $t_{1/2}$ ) of <sup>137</sup>Cs is 30 years. Hence, 500 GBq would be reduced to 445 GBq in five years, i.e., the loss due to radioactive decay in five years is approximately 11%. This reduction is less than the uncertainty in the actual size of the yearly discharges, which is estimated to be between 370 GBq and 500 GBq per year. However, this simplification may also lead to an overestimation of the <sup>137</sup>Cs concentrations in cod and capelin.

The simulations indicated that five years was sufficient to attain a stable maximum concentration close to the source of the continuous discharges (Experiment A). Similarly, this time frame was sufficient to attain maximum overlap estimates with fish distributions for the pulse releases (Experiment B). The time frame of 5 years in Experiments A and B are chosen based on these simulations.

We do not have the same detailed fish distribution data from the eastern Barents Sea as those for farther western regions, which may result in an underestimation of the overlap. The fish survey data represent snapshots of the distributions at the time of the survey. The seasonal timing of the survey in combination with the migration of the fish constrains the scope for coupling of the model and fish distribution data.

In order to calculate the <sup>137</sup>Cs concentrations in cod and capelin we have used CFs based on field measurements in samples collected in the Barents Sea, representing an equilibrium state. In our calculations, we have assumed that the level of <sup>137</sup>Cs in cod and capelin is in equilibrium with its surroundings. This is, however, not a realistic situation short time after an accidental release. Our assumption brings with it uncertainties, both with respect to the uptake from seawater and food. Unfortunately, we do not have sufficient knowledge about the uncertainties to address this point at this time.

#### 4.3. Dispersion from Komsomolets and K-159 vs. dispersion from other point sources

By simply examining the fish data for cod and capelin and the maps showing the dispersal of radioactive substances from *Komsomolets* and *K-159*, it is clear that none of these scenarios represent the worst case for contaminating marine resources in the Barents Sea. From what is known concerning inflow to the Barents Sea (Loeng et al., 1997; Ingvaldsen et al., 2007), it seems obvious that a worst-case scenario would be a pulse release of radioactivity in an area to the southwest of the Barents Sea. During a short time period, such a release would flush an area representing a major part of the Barents Sea ecosystem.

#### 4.4. Impact assessments

A pulse discharge is sensitive to the time of release within the year of release and over time. However, continuous discharges are generally dominated by large-scale features and should be less sensitive to the time of release. Variations in immediate and long-term dispersal are affected by temporal variations in both horizontal velocities and vertical diffusion. Clearly, horizontal velocities change with depths, and the results are therefore dependent on reliable vertical mixing (Fiksen et al., 2007; Vikebø et al., 2007).

A numerical tool able to recapture observed features of long-term leakages may also be used in an operational mode. Introducing ocean forecasts into the model system enables a real-time assessment of spatiotemporal distributions (Vikebø et al., 2011). This approach may be utilised for management purposes when evaluating the risk of contamination of marine resources after a spill of radioactive substances. In addition, when observed in field, such a tool could potentially be used to track the sources of high radioactivity levels. Several studies have reported on the possibility of back-tracking tracers in the ocean from the observational point to the potential source (e.g., Batchelder, 2006; Christensen et al., 2007). Characteristics of the tracer (e.g., composition and half-life) can be valuable contributors to the identification of the source.

## 5. Conclusions

Our results indicate that continuous leakages and pulse discharges from *Komsomolets*, lying at a depth of 1655 m southwest of Bear Island in the Norwegian Sea, induce negligible activity concentrations in muscle of Northeast Arctic cod and whole-body capelin. The same result applies for continuous leakages of  $^{137}\text{Cs}$  from the nuclear submarine wreck *K-159*, lying outside of the Murmansk Fjord at a depth of 238 m, with the exception of the immediate vicinity of the submarine. A pulse discharge of 100% of the  $^{137}\text{Cs}$ -inventory from *K-159* will, on the other hand, result in activity concentrations in muscle of cod exceeding 100 times the present level for approximately two years after the discharge. It is clear that discharges from *Komsomolets* and *K-159* do not represent the worst case for contaminating marine resources in the Barents Sea. A worst-case scenario would probably be a pulse release in an area to the southwest of the Barents Sea. During a short time period, such a release would flush an area representing a major part of the Barents Sea ecosystem.

## References

- Alfimov, V., Possnert, G., Aldahan, A., 2006. Anthropogenic iodine-129 in the Arctic Ocean and Nordic Seas: numerical modeling and prognoses. *Marine Pollution Bulletin* 52, 380–385.
- AMAP, 2009. Arctic Pollution (2009). Arctic Monitoring and Assessment Programme, Oslo, p. xi+83.
- Amundsen, I., Iosjpe, M., Reistad, O., Lind, B., Gussgaard, K., Strand, P., Borghuis, S., Sickel, M., Dowdall, M., 2002. The accidental sinking of the nuclear submarine, the Kursk: monitoring of radioactivity and the preliminary assessment of the potential impact of radioactive releases. *Marine Pollution Bulletin* 44, 459–468.
- Avery, S.V., 1996. Fate of caesium in the environment: distribution between the abiotic and biotic components of aquatic and terrestrial ecosystems. *Journal of Environmental Radioactivity* 30 (2), 139–171.
- Batchelder, H.P., 2006. Forward-in-time/backward-in-time-trajectory (FITT/BITT) modeling of particles and organisms in the coastal ocean. *Journal of Atmospheric and Oceanic Technology* 23, 727–741.
- Baxter, M.S., Harms, I., Osvath, I., Povinec, P.P., Scott, E.M., 1998. Modelling the potential radiological consequences of radioactive waste dumping in the Kara Sea. *Journal of Environmental Radioactivity* 39, 161–181.
- Bergstad, O.A., Jørgensen, T., Dragesund, O., 1987. Life history and ecology of the gadoid resources of the Barents Sea. *Fisheries Research* 5, 119–161.
- Blindheim, J., Føyn, L., Martinsen, E.A., Svendsen, E., Sætre Hjøllo, S., Adlandsvik, B., 1994. In: Sætre, R. (Ed.), *The Sunken Nuclear Submarine in the Norwegian Sea – a Potential Environmental Problem?* Fiksen og Havet 7.
- Bretton, M., Salomon, J.C., 1995. A 2D long term advection – dispersion model for the Channel and Southern North Sea. Part A: validation through comparison with artificial radionuclides. *Journal of Marine Systems* 6, 495–513.
- Christensen, A., Daewel, U., Jensen, H., Moosegaard, H., St John, M., Schrum, C., 2007. Hydrodynamic backtracking of fish larvae by individual-based modelling. *Marine Ecology Progress Series* 347, 221–232.
- Dingsør, G.E., 2005. Estimating abundance indices from the international 0-group fish survey in the Barents Sea. *Fisheries Research* 72, 205–218.
- Eriksen, E., Prozorkevic, D., Dingsør, G.E., 2009. An evaluation of 0-group abundance indices of Barents Sea fish stocks. *The Open Fish Science Journal* 2, 6–14.
- Fiksen, Ø., Jørgensen, C., Kristiansen, T., Vikebø, F., Huse, G., 2007. Linking behavioural ecology and oceanography: how larval behaviour determines growth, mortality and dispersal. *Marine Ecology Progress Series* 347, 195–205. <http://dx.doi.org/10.3354/meps06978>.
- Gao, Y., Drange, H., Bentsen, M., Johannessen, O., 2004. Simulating transport of non-Chernobyl  $^{137}\text{Cs}$  and  $^{90}\text{Sr}$  in the North Atlantic-Arctic region. *Journal of Environmental Radioactivity* 71 (1), 1–16.
- Gill, E.A., 1982. *Atmosphere–Ocean Dynamics*. Academic Press.
- Gjøsæter, H., Dommasnes, A., Røttingen, B., 1998. The Barents Sea capelin stock 1972–1997. A synthesis of results from acoustic surveys. *Sarsia* 83, 497–510.
- Gladkov, G.A., Sivintsev, Yu. V., 1994. Radiation conditions near the sunken submarine “Komsomolets”. *Atomic Energy* 77 (5), 865–871.
- Gwynn, J.P., Heldal, H.E., Gäfvert, T., Blinova, O., Eriksson, M., Sværen, I., Brungot, A.L., Strålberg, E., Møller, B., Rudjord, A.L., 2012. Radiological status of the marine environment of the Barents Sea. *Journal of Environmental Radioactivity* 113, 155–162.
- Haidvogel, D., Arango, H., Budgell, W., Cornuelle, B., Curchitser, E., Lorenzo, E.D., Fennel, K., et al., 2008. Ocean forecasting in terrain-following coordinates: formulation and skill assessment of the regional ocean modelling system. *Dynamics of Atmospheres and Oceans* 227, 3595–3624.
- Hallstadius, L., Garcia-Montaña, E., Nilsson, U., Boelskifte, S., 1987. An improved and validated dispersion model for the North Sea and adjacent waters. *Journal of Environmental Radioactivity* 5, 261–274.
- Hansen, C., Samuelsen, A., 2009. Influence of horizontal model grid resolution on the simulated primary production in an embedded primary production model in the Norwegian Sea. *Journal of Marine Systems* 75 (1–2), 236–244.
- Hamre, J., 1994. Biodiversity and exploitation of the main fish stocks in the Norwegian – Barents Sea ecosystem. *Biodiversity and Conservation* 3, 473–492.
- Heldal, H.E., Varskog, P., Føyn, L., 2002. Distribution of selected anthropogenic radionuclides ( $^{137}\text{Cs}$ ,  $^{238}\text{Pu}$ ,  $^{239,240}\text{Pu}$  and  $^{241}\text{Am}$ ) in marine sediments with emphasis on the Spitsbergen-Bear Island area. *The Science of the Total Environment* 293, 233–245.
- Heldal, H.E., Føyn, L., Varskog, P., 2003. Bioaccumulation of Cs-137 in pelagic food webs in the Norwegian and Barents Seas. *Journal of Environmental Radioactivity* 65 (2), 177–185.
- Hermansen, K., Selnæs, Ø., Eikermann, I.M., Holo, E., Liland, A., Sickel, M., Amundsen, I., Reistad, O., 2006. *K-159. Havariet av den russiske atomubåten K-159 og den norske atombredskapsorganisasjonens håndtering av ulykken. StrålevernRapport 2006:8. Statens strålevern, Østerås (in Norwegian)*.
- Høibråten, S., Haugan, A., Thoresen, P., 2003. *The Environmental Impact of the Sunken Submarine Komsomolets. FFI/Report-2003/02523. Norwegian Defence Research Establishment*, p. 41.
- Høibråten, S., Thoresen, P.E., Haugan, A., 1997. The sunken nuclear submarine Komsomolets and its effects on the environment. *The Science of the Total Environment* 202 (1–3), 67–78.
- IAEA, 2004. *Sediment Distribution Coefficients and Concentration Factors for Biota in the Marine Environment. Technical Reports Series No. 422. International Atomic Energy Agency, Vienna, Austria*.
- Ingvaldsen, R., Asplin, L., Loeng, H., 2007. The seasonal cycle in the Atlantic transport to the Barents Sea during the years 1997–2001. *Continental Shelf Research* 24, 1015–1032.
- Jakobsen, T., Korsbrekke, K., Mehl, S., Nakken, O., 1997. Norwegian Combined Acoustic and Bottom Trawl Surveys for Demersal Fish in the Barents Sea During Winter. ICES Document CM 1997/Y: 17, p. 26.
- Karcher, M.J., Gerland, S., Harms, I.H., Iosjpe, M., Heldal, H.E., Kershaw, P., Sickel, M., 2004. The dispersion of  $^{99}\text{Tc}$  in the Nordic Seas and the Arctic Ocean: a comparison of model results and observations. *Journal of Environmental Radioactivity* 74, 185–198.
- Kershaw, P., Baxter, A., 1995. The transfer of reprocessing wastes from north–west Europe to the Arctic. *Deep-Sea Research Part 2* 42 (6), 1413–1448.
- Loeng, H., Ozhigin, V., Adlandsvik, B., 1997. Water fluxes through the Barents Sea. *ICES Journal of Marine Science* 54, 310–317.
- NRPA, 2011. *Radioactivity in the Marine Environment 2008 and 2009. Results from the Norwegian National Monitoring Programme (RAME). StrålevernRapport 2011:4. Norwegian Radiation Protection Authority, Østerås*.
- Olsen, E., Aanes, S., Mehl, S., Holst, J.C., Aglen, A., Gjøsæter, H., 2010. Cod, haddock, saithe, herring, and capelin in the Barents Sea and adjacent waters: a review of the biological value of the area. *ICES Journal of Marine Science* 67, 87–101.
- Orre, S., Gao, Y., Drange, H., Nilsen, J.E.Ø., 2007. A reassessment of the dispersion properties of  $^{99}\text{Tc}$  in the North Sea and the Norwegian Sea. *Journal of Marine Systems* 68, 24–38.
- Ramsden, D., Holloway, G., 1991. Timestepping Lagrangian particles in two dimensional Eulerian flow fields. *Journal of Computational Physics* 95, 101–111.
- Sakshaug, E., Bjørge, A., Gulliksen, B., Loeng, H., Mehlum, F., 1994. Structure, biomass distribution, and energetics of the pelagic ecosystem in the Barents Sea: a synopsis. *Polar Biology* 14, 405–411.
- Schönfeld, W., 1995. Numerical simulation of the dispersion of artificial radionuclides in the English Channel and the North Sea. *Journal of Marine Systems* 6, 529–544.
- Smith, J.N., Ellis, K.M., Kilius, L.R., 1998. I-129 and Cs-137 tracer measurements in the Arctic Ocean. *Deep-Sea Research Part 1* 45 (6), 959–984.
- Thygesen, U.H., Adlandsvik, B., 2007. Simulating vertical turbulent dispersal with finite volumes and binned random walks. *Marine Ecology Progress Series* 347, 145–153.
- Vikebø, F.B., Husebø, Å., Slotte, A., Stenevik, E.K., Lien, V.S., 2010. Impact of hatching date, vertical distribution and inter-annual variation in physical forcing on northward displacement and temperature conditions of Norwegian spring spawning herring larvae (*Clupea harengus* L.). *ICES Journal of Marine Science* 67, 1710–1717.
- Vikebø, F., Jørgensen, C., Kristiansen, T., Fiksen, Ø., 2007. Drift, growth and survival of larval Northeast Arctic cod with simple rules of behaviour. *Marine Ecology Progress Series* 347, 207–219. <http://dx.doi.org/10.3354/meps06979>.
- Vikebø, F.B., Adlandsvik, B., Albretsen, J., Sundby, S., Stenevik, E.K., Huse, G., Kristiansen, T., Eriksen, E., 2011. Real time ichthyoplankton drift in Northeast Arctic cod and Norwegian spring spawning herring. *PLoS ONE* 6, e27367.
- Westgård, T., Johansen, G.O., Kvamme, C., Adlandsvik, B., Stiansen, J.E., 2010. A framework for storing, retrieving and analysing marine ecosystem data of different origin with variable scale and distribution in time and space. In: Nishida, T., Caton, A.E. (Eds.), *2010. GIS/Spatial Analyses in Fishery and Aquatic Sciences*, vol. 4. International Fishery GIS Society, Saitama, Japan, ISBN 4-9902377-2-2, pp. 417–432.